

Drug Analysis & Pharmacokinetics and Drug Formulation, DDS Research Laboratories, Pharmaceutical Research Division, Takeda Chemical Industries Ltd, 2-17-85 Jusohonmachi, Yodogawa-ku, Osaka 532-8686, Japan

Yasuyuki Suzuki, Katsumi Iga, Shigeo Yanai, Yukihiro Matsumoto, Yasuaki Ogawa

Pharmaceutical Research Laboratories, Pharmaceutical Research Division, Takeda Chemical Industries Ltd, 2-17-85 Jusohonmachi, Yodogawa-ku, Osaka 532-8686, Japan

Masahiro Kawase, Tunehiko Fukuda

Tsukuba Research Laboratories, Hisamitsu Pharmaceutical Co. Inc., 1-25-11 Kannondai, Tsukuba, Ibaraki 305-0856, Japan

Hirotochi Adachi, Naruhito Higo

Correspondence: Y. Suzuki, DDS Research Laboratories, Pharmaceutical Research Division, Takeda Chemical Industries Ltd, 2-17-85 Jusohonmachi, Yodogawa-ku, Osaka 532-8686, Japan.

Acknowledgments: We gratefully acknowledge Dr K. Okabe of Advance Co. for advice in iontophoresis, and the following people of Takeda Chemical Ind. Ltd for their contributions: Mrs M. Nakamura for her assistance; Mr T. Asano, Drs H. Sawada and O. Nishimura for their supply of hPTH(1–34); and Drs S. Taketomi and Y. Igari for their fruitful discussion.

Iontophoretic pulsatile transdermal delivery of human parathyroid hormone (1–34)

Yasuyuki Suzuki, Katsumi Iga, Shigeo Yanai, Yukihiro Matsumoto, Masahiro Kawase, Tunehiko Fukuda, Hirotochi Adachi, Naruhito Higo and Yasuaki Ogawa

Abstract

Iontophoretic pulsatile transdermal delivery of hPTH(1–34) was examined in Sprague-Dawley (SD) rats, hairless rats and beagle dogs. Application for 60 min (200 μg ; 0.1 mA cm^{-2}) showed current-responsive increases in serum hPTH(1–34) levels in all the animals. In SD rats, the area under the curves of serum hPTH(1–34) levels (AUCs) were proportional to the doses (40, 120, 200, 400 and 1000 μg) and current densities (0.05, 0.1 and 0.15 mA cm^{-2}) applied. The absorption rates per 200- μg dose, calculated by a deconvolution method, were 6.7, 2.4 and 3.7 $\mu\text{g h}^{-1}$ for SD rats, hairless rats and beagle dogs, respectively. These values correlated well with the ratios of the skin porosity to the dermal thickness reported for these animals, which are believed to represent the reciprocal of the electrical resistance of the aqueous channels formed by the hair follicles. From this correlation, we suggested that absorption of hPTH(1–34) occurs mainly via the hair-follicle route, and that the absorption rate in man might be intermediate between those in hairless rats and beagle dogs. Three-fold repetitions of 30 min current with various rest intervals produced current-responsive triple pulses in serum hPTH(1–34) levels in SD rats. Seven-fold repetitions of current also produced similar current-responsive pulsatile serum hPTH(1–34) levels. However, peak serum hPTH(1–34) levels tended to decrease gradually after the fourth current application, possibly due to consumption of the electrodes, suggesting that three-fold repetitions of current might be optimal. These findings suggest that this iontophoretic administration system could create a repeated-pulsatile pattern of serum hPTH(1–34) levels without the necessity for frequent injections, and may be useful for the treatment of osteoporosis with hPTH(1–34).

Introduction

Human parathyroid hormone (1–34), hPTH(1–34), is an active fragment of the full-length peptide, hPTH(1–84). These hormones have both anabolic and catabolic effects on bone (Dempster et al 1993) and frequent intermittent administration is known to enhance their anabolic and anti-osteoporotic effects (Tam et al 1982; Hock et al 1992; Riond 1993; Kawase et al 1994; Uzawa et al 1995). Therefore, pulsatile administration might be useful for the treatment of osteoporosis (Reeve 1996; Lindsay 1997).

Clinical studies with parathyroid hormones have been carried out using once-weekly or daily injections (Sone et al 1995). However, this route of administration is not suitable for self-medication and the high frequency of injections is

uncomfortable and inconvenient for patients. In healthy subjects, parathyroid hormones are known to be secreted by the parathyroid gland in a periodic pulsatile manner (Harrms et al 1989). Delivering hPTH(1–34) in a way that mimics this secretion pattern might increase efficacy without compromising effects. Thus we focused our research on pulsatile delivery of hPTH(1–34) by iontophoresis.

Iontophoresis is a technique that uses a low-level electric current to enhance transdermal drug delivery (Banga & Chien 1993; Green 1996; Riviere & Heit 1997). In principle, it allows molecules which are unable to diffuse passively through the skin to permeate the skin barrier by electrophoresis or electro-osmosis (particularly for large molecules; Guy et al 2000). Since hPTH(1–34) is positively charged and has a lower molecular weight (about 4000) than insulin (about 6000), which is thought to be the largest molecule that can undergo transdermal iontophoretic delivery (Banga et al 1999), we considered it a suitable candidate for iontophoretic delivery. This technique is particularly beneficial for the delivery of hPTH(1–34) since it can produce pulsatile drug absorption in response to the programmed current.

The purposes of this study were threefold: to examine the iontophoretic pulsatile transdermal delivery of hPTH(1–34) using animal models; to compare absorption rates in different animals to predict the absorption rate in humans; and to find the maximally achievable number of pulses in serum hPTH(1–34) levels by on-and-off current application.

Materials and Methods

hPTH(1–34)

Powdered hPTH(1–34) hydrochloride (relative purity as analysed by HPLC, higher than 99%) was obtained from Discovery Research Laboratories, Takeda Chemical Ind. Ltd, and was produced by fragmenting recombinant hPTH(1–84) (Nakagawa et al 1994).

Animals

For administration experiments, 7-week old male Sprague-Dawley (SD) rats weighing about 250 g (Clea Japan), 7-week old male HWY hairless rats weighing about 200 g (SLC Japan) and male beagle dogs weighing about 10 kg (Toyo Beagle) were used. The studies were carried out in accordance with the Guide for the Care and Use of Laboratory Animals adopted by the Committee of Animal Care at Takeda Chemical Industries.

Dosage form

For intravenous and subcutaneous administration, aqueous solutions of hPTH(1–34), 2 and 8 $\mu\text{g mL}^{-1}$ kg^{-1} , were prepared by dissolving hPTH(1–34) in saline containing 0.5% bovine serum albumin.

For iontophoretic administration, the hydrogel layers of the electrode units are thought to be important because they are essential for maintaining conductivity during current application (Banga & Chien 1993). In a preliminary study, we tried to use an anodal patch in which hPTH(1–34) was contained by a hydrogel layer. However, this system was found to require a relatively large amount of hPTH(1–34) to achieve sufficient transdermal delivery and did not guarantee the drug's stability during storage. Therefore, as an improved drug reservoir system, in this study, we used a porous membrane system which contained hPTH(1–34) under dry conditions and was kept separated from a hydrogel layer before use. Upon use, the membrane system and the hydrogel contacted each other so that we could maintain hPTH(1–34) stably during storage and achieve a higher concentration of hPTH(1–34) at the interface between the drug reservoir and the skin.

The patch and device is shown in Figure 1. It consisted of an anodal patch and a cathodal patch that were connected to an electric current controller (ADIS ver. 6) and an electric meter (ADIS tester IV) (Okabe et al 1986). The anodal patch was made up of an electrode unit (electrode plus hydrogel) and a drug-loaded porous membrane (surface area, 9.6 cm^2 ; Millipore) containing hPTH(1–34) at concentrations of 40–1000 $\mu\text{g}/\text{membrane}$ under dry conditions. The hydrogel was prepared by using 1% agar with citrate buffer (pH 5). The drug-loaded membrane was prepared by applying hPTH(1–34) aqueous solution at concentration of 40–1000 $\mu\text{g}/50 \mu\text{L}$ on the porous membrane. The electrode unit and the drug-loaded porous membrane were kept separated before administration. At the start of administration, they were held in contact with each other with adhesive tape. The electrode unit was composed of a silver electrode sheet and a conductive hydrogel layer weighing about 1.4 g. They were housed in a plastic cup (i.d., 30 mm; thickness, 1.5 mm). The cathodal patch was composed of a silver–silver chloride electrode sheet and an adhesive conductive hydrogel layer.

Intravenous and subcutaneous administration

SD and HWY hairless rats were anaesthetized with intraperitoneal pentobarbital (initial dose, 0.4 mg kg^{-1})

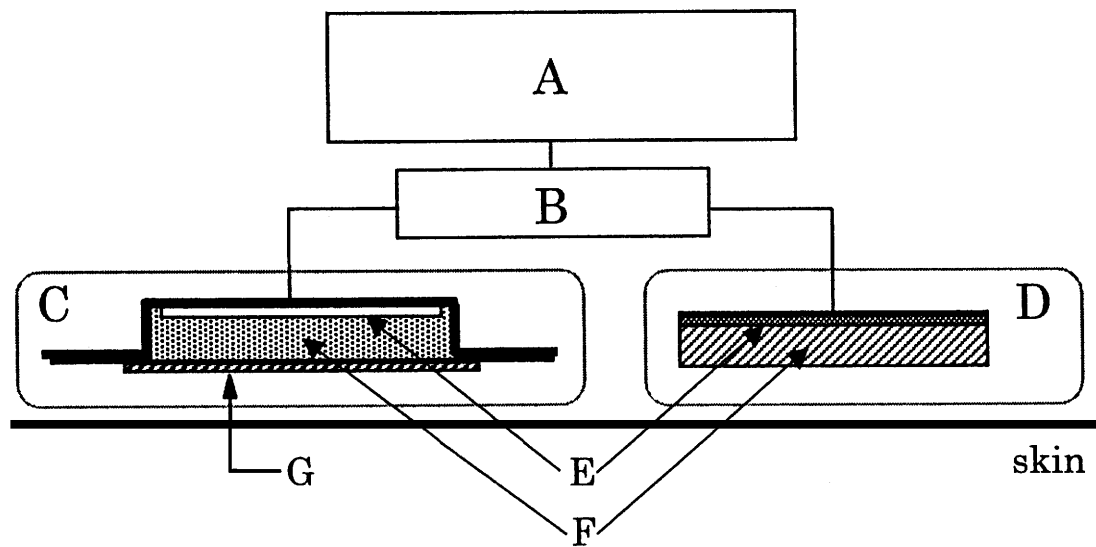


Figure 1 Iontophoretic administration device consisting of an anodal patch and a cathodal patch that are connected to an electric current controller and an electric meter. A, power generator (ADIS); B, ADIS tester (electric meter); C, anodal patch; D, cathodal patch; E, electrode; F, conductive hydrogel; G, drug-loaded porous membrane.

and were kept lying on their backs on a plate with their legs fastened. The intravenous dose was given via the right (or left) jugular vein, whereas the subcutaneous dose was given on the neck. Beagle dogs were fastened in a rack without anaesthesia. The intravenous dose was given via the right (or left) leg vein, whereas the subcutaneous dose was given on the side.

Iontophoretic administration

SD and hairless rats were kept anaesthetized with ethyl ether for shaving and positioning of the patches, and thereafter they were held in a constraining cage without anaesthesia (Ballman cage, Natsume). Beagle dogs were fastened in a rack without anaesthesia. The administration site (abdomen for SD and hairless rats; the side for beagle dogs) was shaved with a hair clipper (NP-3B, Shimazu Denki) and a shaver (Braun system 1-2-3, Braun) and then wiped with a piece of cotton wool soaked in 75% alcohol. Then, the anodal and cathodal patches were placed, separated by about 2 cm, and fixed into position on the skin, with an elastic bandage (Silkytex, Alcare). The anodal and cathodal patches were connected to an electric controller and an electric meter.

A depolarizing pulsatile direct current of 50 kHz and 50% duty was applied for each administration. The

current density was maintained at 0.05, 0.1 or 0.15 mA cm⁻² on the basis of the average intensity of the forward and backward currents throughout the cycle per unit surface area. For single-pulse administration, current was applied for 60 min. For multiple-pulse administration, a 20-min or 30-min current application was repeated with rest intervals of 40, 60 or 90 min.

Measurement of serum hPTH(1-34) levels

Blood samples (about 0.3 mL) were taken with a syringe at appropriate time intervals after administration: about 0.3 mL from the vein in SD and hairless rats, and about 1.0 mL from the leg vein in beagle dogs. In intravenous administration experiments, blood samples were taken from veins away from the injection site, avoiding drug contamination. Samples were left to stand for at least 1 h in an ice box, then centrifuged at 12 000 rev min⁻¹ for 10 min at 4°C. The resulting serum samples (about 0.1 mL) were kept in Teflon-coated plastic tubes at -40°C until assay. Serum hPTH(1-34) levels were measured by RIA using a rat PTH kit (Nichols Institute), which has been ascertained to be also valid for the assay of hPTH(1-34). Before the measurement, serum samples were diluted with an appropriate volume of albumin-containing dilution solution that was supplied with the kit.

Pharmacokinetic analysis

The serum hPTH(1–34) levels after intravenous administration of hPTH(1–34) were fitted to a bi-exponential function:

$$A \exp(-\alpha t) + B \exp(-\beta t) \quad (1)$$

The area under the curve of serum hPTH(1–34) level (AUC) and the total body clearance (CL_t) after intravenous administration were calculated as:

$$AUC_{iv} = A/\alpha + B/\beta \quad (2)$$

where $CL_t = \text{Dose}/AUC_{iv}$. The AUC after subcutaneous administration or iontophoretic administration of hPTH(1–34) was calculated by the trapezoidal rule. The bioavailability for subcutaneous administration or iontophoretic administration was calculated using the AUC_{iv} obtained after dose compensation as a reference standard. Time-dependent transdermal absorption rates after iontophoretic administration were calculated by a deconvolution method (Iga et al 1986), by assuming that a characteristic response function after impulse input is equal to the bi-exponential function obtained in intravenous administration. The mean absorption rates were calculated by averaging the time-dependent absorption rates obtained at time points over 30–60 min.

Results and Discussion

Pharmacokinetics of hPTH(1–34) after intravenous and subcutaneous administration

Serum hPTH(1–34) levels after intravenous and subcutaneous administration to SD and HWY rats and beagle dogs are shown in Figure 2. The serum hPTH(1–34) level after intravenous administration decreased rapidly in all cases. The levels were fitted to a bi-exponential equation (equation 1). The values of A, B, α , β , AUC and CL_t are listed in Table 1. The CL_t in SD rats was almost double that in hairless rats and beagle dogs. The values of A, B, α , and β were used for the calculation of absorption rates in iontophoresis.

With subcutaneous administration, the serum hPTH(1–34) level reached a peak within 30 min in all animals (time to peak level was 15 min in SD and hairless rats and 30 min in beagle dogs) and thereafter decreased gradually. The bioavailability following subcutaneous administration was similar in the three species (Table 1; about 60%), suggesting that the residual amount (40%) was eliminated from the subcutaneous tissues and that this type of elimination might occur during iontophoretic administration.

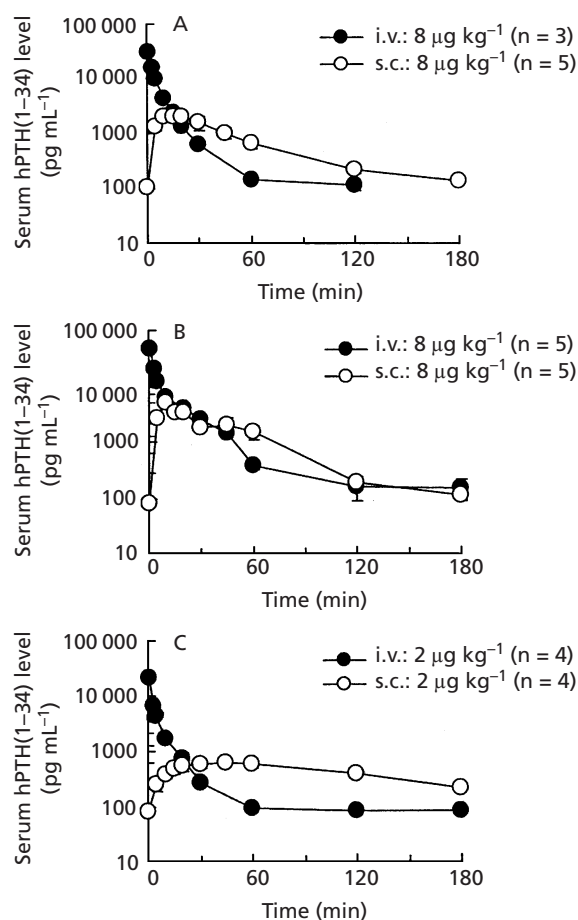


Figure 2 Serum hPTH(1–34) levels after intravenous and subcutaneous administration of hPTH(1–34) to SD rats (dose, $8 \mu\text{g kg}^{-1}$; A), hairless rats (dose, $8 \mu\text{g kg}^{-1}$; B) and beagle dogs (dose, $2 \mu\text{g kg}^{-1}$; C). Each point represents the mean \pm s.e.m. (no. of animals is shown in parenthesis).

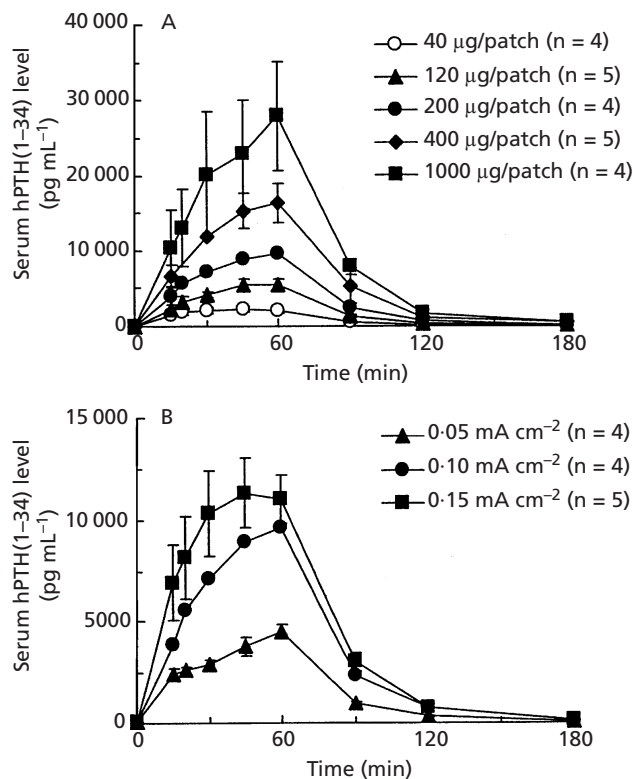
Iontophoretic transdermal absorption of hPTH(1–34)

Figure 3A shows serum hPTH(1–34) levels in SD rats during and after 60-min application of a current of 0.1 mA cm^{-2} with various applied doses (40–1000 μg /patch). The peak serum hPTH(1–34) level increased with duration of current and with dose applied, and the maximal serum levels appeared near the end of the current application. The AUCs were almost proportional to the applied doses. The average bioavailability for the applied doses (40, 120, 200, 400 and 1000 μg /patch) at 0.1 mA cm^{-2} in SD rats was about 3.6%.

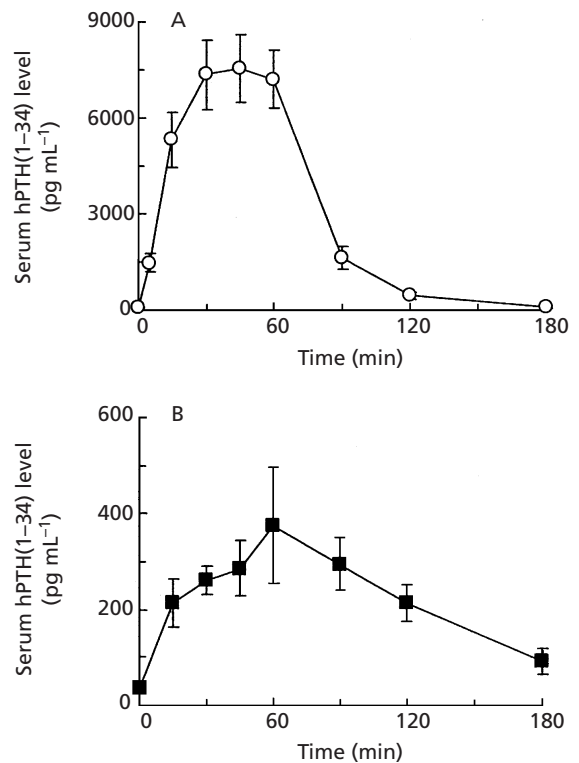
Figure 3B shows serum hPTH(1–34) levels in SD rats during and after 60 min application of a current of 0.05,

Table 1 Pharmacokinetic parameters obtained from intravenous and subcutaneous administration of hPTH(1–34) to SD rats, hairless rats and beagle dogs.

	SD rat	Hairless rat	Beagle dog
Body weight (kg)	0.26	0.22	9.6
Dose ($\mu\text{g kg}^{-1}$)	8	8	2
A (ng mL^{-1})	33.9	67.2	42.7
B (ng mL^{-1})	12.0	9.9	6.9
α (h^{-1})	30.8	33.8	62.1
β (h^{-1})	6.6	2.8	7.7
AUC ($\text{ng}\cdot\text{h mL}^{-1}$)	2.92	5.57	1.58
CL_t ($\text{L h}^{-1} \text{kg}^{-1}$)	2.74	1.44	1.27
Bioavailability (s.c. (%))	57.3	56.7	67.4

**Figure 3** Serum hPTH(1–34) levels during and after iontophoretic administration of hPTH(1–34) to SD rats. A. Dose responsiveness (current application time, 60 min; applied current density, 0.1 mA cm^{-2} ; applied doses, 40, 120, 200, 400 and $1000 \mu\text{g/patch}$). B. Current responsiveness (applied current density, 0.05, 0.10 and 0.15 mA cm^{-2} ; current application time, 60 min; applied dose, $200 \mu\text{g/patch}$). Each point represents the mean \pm s.e.m. (no. of animals is shown in parenthesis).

0.1 and 0.15 mA cm^{-2} with $200 \mu\text{g/patch}$. The peak serum level increased with the current density. The AUC was almost proportional to the applied current density.

**Figure 4** Serum hPTH(1–34) levels during and after iontophoretic administration of hPTH(1–34) to hairless rats (A; $n = 5$) and beagle dogs (B; $n = 4$) (current application time, 60 min; applied current density, 0.1 mA cm^{-2} ; applied dose, $200 \mu\text{g/patch}$). Each point represents the mean \pm s.e.m.

The serum hPTH(1–34) levels upon application of a hPTH(1–34) patch without electronic current were also examined. However, the serum hPTH(1–34) levels were very low, suggesting that the passive permeation of hPTH(1–34) was negligible (data not shown). Our preliminary experiments on current application in humans suggested that the highest tolerable current density might be 0.1 mA cm^{-2} . Therefore, we mainly used this current density in later experiments.

Figure 4 shows serum hPTH(1–34) levels during and after 60 min application of current in hairless rats and beagle dogs ($200 \mu\text{g/patch}$). As in SD rats, the serum level increased rapidly in response to the current and the maximal serum levels appeared near the end of the application period.

The peak serum level obtained in hairless rats was equivalent to that in SD rats at the same applied dose ($200 \mu\text{g/patch}$). However, the absorption in hairless rats is expected to be about half that in SD rats, since the CL_t of hPTH(1–34) in hairless rats was half that in SD rats (Table 1).

Comparison of current-responsive transdermal absorption rates in different animals

To estimate the transdermal absorption rates during current application, we calculated time-dependent absorption rates by the deconvolution method. Figure 5 shows a typical time-dependent absorption rate profile in SD rats with 200 $\mu\text{g}/\text{patch}$ and a current density 0.1 mA cm^{-2} . The absorption rate increased rapidly with time, approaching a quasi-steady-state value until the end of the current application and thereafter decreased rapidly. Similar time-dependent absorption rate profiles were obtained in hairless rats and beagle dogs (200 $\mu\text{g}/\text{patch}$). The mean absorption rates (mean \pm

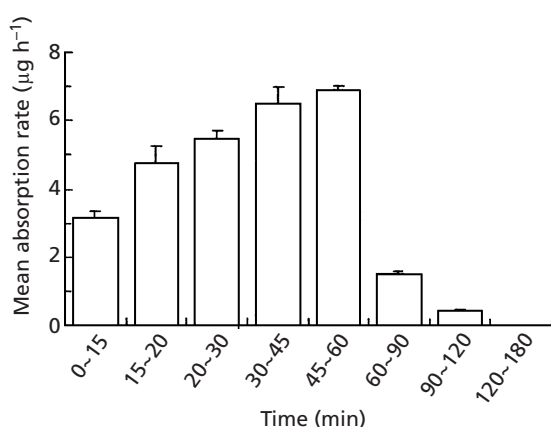


Figure 5 Time-dependent transdermal absorption rates calculated by a deconvolution method (Iga et al 1986) for the iontophoretic administration of hPTH(1-34) to SD rats (current application time, 60 min; applied current density, 0.1 mA cm^{-2} ; applied dose, 200 $\mu\text{g}/\text{patch}$). Each point represents the mean \pm s.e.m.

s.e.m.; 200 $\mu\text{g}/\text{patch}$) in SD rats, hairless rats and beagle dogs were 6.7 ± 0.3 , 3.7 ± 1.1 and $2.4 \pm 0.3 \mu\text{g h}^{-1}$, respectively. SD rats exhibited the highest value and hairless rats exhibited the lowest value.

For iontophoretic transdermal absorption, two routes are available: the aqueous pore route, and the stratum corneum transport route (Riviere & Heit 1997); the former may be explained by aqueous channels formed by the hydrated hair follicle (hair-follicle route, possibly in animals used in this study) or the hydrated hair follicle plus the sweat gland (hair-follicle/sweat-gland route, possibly in humans). It is assumed that the barrier of the stratum corneum is too tight to achieve effective transport of a large hydrophilic molecule and therefore that the aqueous pore route will prevail for hPTH(1-34) (Bath et al 2000). By analogy to the transport of electrical current through a hydrated porous membrane, the magnitude of drug transport via the aqueous pore route is assumed to be proportional to the reciprocal of the resistance of the aqueous pore, which in turn is proportional to the ratio of skin porosity to the depth of the aqueous channels. Thus, interspecies differences in the magnitude of drug transport can be explained by differences in the ratio of skin porosity to the depth of the aqueous channels. Assuming the hair-follicle route applies, the skin porosity can be represented by the porosity calculated from the total surface area occupied by the hair follicles on the skin surface while the depth of the aqueous channels can be represented by epidermal thickness (the thickness of the stratum corneum plus the epidermis). Table 2 shows skin anatomy parameters and the ratio of hair-follicle-associated skin porosity to epidermal thickness in various species (based on early reports; Bronaugh et al 1982; Al-Bagdadi & Lovell 1985;

Table 2 Skin anatomy and the ratio of skin porosity to epidermal thickness in various animals

	SD rat	Hairless rat	Beagle dog	Human
Hair-follicles				
Number (cm^{-2})	342 ^a	17 ^b	96 ^a	11 ^a
Diameter (μm)	25 ^c	25 ^b	25 ^d	97 ^c
Skin porosity (%) ^e	0.168	0.008	0.047	0.081
Dermal thickness (μm)				
Stratum corneum	4.3 ^a	6.5 ^b	5 ^a	18.4 ^a
Epidermis	14.7 ^a	29.4 ^b	16.7 ^a	49.5 ^a
Total	19.0 ^a	36.0 ^b	21.7 ^a	67.9 ^a
Ratio of skin porosity to dermal thickness (% mm^{-1})	11.42	0.28	3.78	1.64

^aPanchagnula et al (1997); ^bItagaki et al (1995); ^cBronaugh et al (1982); ^dAl-Bagdadi & Lovell (1985); ^eskin porosity (%) = $(\text{diameter}/2)^2 \times \pi \times (\text{number}) \times 100$.

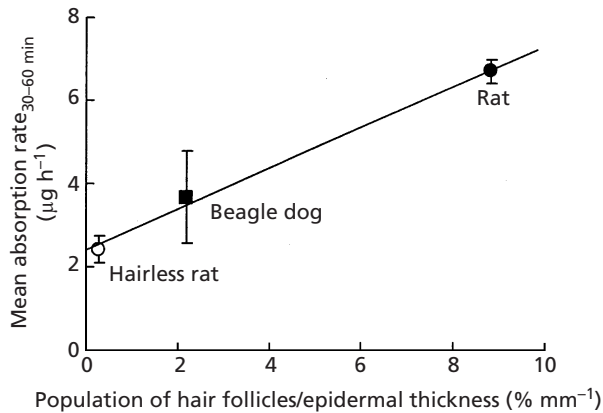


Figure 6 Relationship between mean absorption rate (the average of time-dependent absorption rates obtained at time points from 30 to 60 min) and the ratios of skin porosity to dermal thickness in SD rats, hairless rats and beagle dogs. Each mean absorption rate represents the mean \pm s.e.m. Regression line: mean absorption rate ($\mu\text{g h}^{-1}$) = $0.49 \times$ skin porosity/epidermal thickness ($\% \text{ mm}^{-1}$) + 2.42, $r = 0.997$.

Itagaki et al 1995; Panchagnula et al 1997); the ratio of skin porosity to epidermal thickness in humans takes an intermediate value (1.6) between the values obtained in hairless rats and beagle dogs. Figure 6 shows that there is a good correlation between the absorption rate and the ratio of skin porosity to epidermal thickness in SD rats, hairless rats and beagle dogs. This good correlation suggests that the hair follicle may be a common main route for the transdermal iontophoretic delivery of hPTH(1–34) in all kinds of species and that, from this relationship, the absorption rate of hPTH(1–34) via the hair-follicle route in humans can be predicted to take an intermediate value between the values obtained in hairless rats and beagle dogs (the absorption rate of hPTH(1–34) might be larger on an assumption of hair-follicle/sweat-gland route). This information might be useful for setting an initial dose of hPTH(1–34) in future clinical studies.

Repeated-pulsatile pattern of serum hPTH(1–34) levels after multiple-pulse iontophoretic administration

Figure 7A shows the current-responsive pulsatile serum hPTH(1–34) levels in SD rats during seven-fold repetitions of 20 min of current with rest intervals of 40 min. The serum hPTH(1–34) level increased and decreased in response to the current on and off period. A maximum seven peaks could be created by repetitions of current. However, the peak serum level tended to decrease gradually after the fourth current application (possibly due to

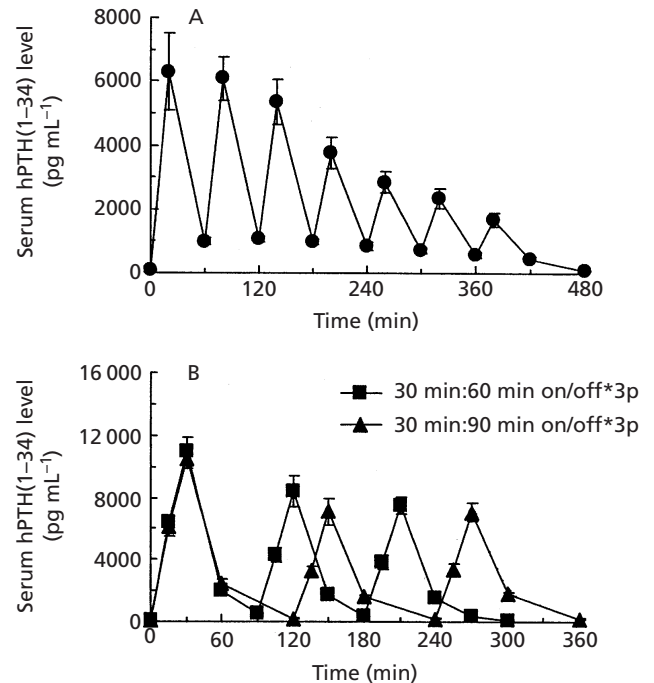


Figure 7 Current-responsive pulsatile serum hPTH(1–34) levels in SD rats during seven-fold repetitions of 20 min of current with rest intervals of 40 min ($n = 5$) (A) and three-fold repetitions of 30 min of current with rest intervals of 60 min ($n = 5$) or 90 min ($n = 4$) (B) (applied current density, 0.1 mA cm^{-2} ; applied dose, $200 \mu\text{g/patch}$). Each point represents the mean \pm s.e.m.

consumption of the electrodes, as suggested by the rapid elevation of the resistance after the fourth current application (data not shown)), suggesting that three cycles of current might be optimal.

Figure 7B shows the current-responsive pulsatile serum hPTH(1–34) levels in SD rats during three-fold repetitions of 30 min of current with rest intervals of 60 or 90 min. Similar current-responsive pulsatile serum hPTH(1–34) levels were obtained. The peak serum levels decreased slightly with time. However, this decrease in the peak seemed not to be dependent on the duration of the rest interval, suggesting that time-dependent decreases in the drug concentration at the interface between the drug reservoir and the skin may be negligible.

Conclusions

In this study, iontophoretic transdermal delivery of hPTH(1–34) was demonstrated in animal models. Absorption-rate analysis in the three types of animals suggested that transdermal absorption of hPTH(1–34) occurs mainly via the hair-follicle route, and that the

absorption rate via the hair-follicle route in humans might be expected to be intermediate between the values obtained in hairless rats and beagle dogs. Three-fold repetitions of a 30-min current with various rest intervals produced current-responsive triple pulses in the serum levels of hPTH(1–34). This method may be useful for the treatment of osteoporosis with hPTH(1–34).

References

- Al-Bagdadi, F., Lovell, J. (1985) Act 3 Integument. In: Evans, H. E., Christensen, G. C. (eds) *Millers Anatomy of the drug*, 2nd edn., pp. 77–98
- Banga, A. K., Chien, Y. W. (1993) Hydrogel-based iontophoretic delivery devices for transdermal delivery of peptide/protein drugs. *Pharm. Res.* **10**: 697–702
- Banga, A. K., Bose, S., Ghosh, T. K. (1999) Iontophoresis and electroporation: comparisons and contrasts. *Int. J. Pharm.* **179**: 1–19
- Bath, B. D., Scott, E. R., Phipps, J. B., White, H. S. (2000) Scanning electrochemical microscopy of iontophoretic transport in hairless mouse skin. Analysis of the relative contributions of diffusion, migration, and electroosmosis to transport in hair follicles. *J. Pharm. Sci.* **89**: 1537–1549
- Bringhurst, F. R., Stern, A. M., Yotts, M., Mizrahi, N., Segre, G. V., Potts, J. T. (1988) Peripheral metabolism of PTH: fate of biologically active amino terminus in vivo. *Am. J. Physiol.* **255**: E886–E893
- Bronaugh, R. L., Stewart, R. F., Congdon, E. R. (1982) Methods for in vitro percutaneous absorption studies II: animal models for human skin. *Toxicol. Appl. Pharmacol.* **62**: 481–488
- Dempster, D. W., Cosman, F., Parisien, M., Shen, V., Lindsay, R. (1993) Anabolic actions of parathyroid hormone on bone. *Endocr. Rev.* **14**: 690–704
- Green, P. G. (1996) Iontophoretic delivery of peptide drugs. *J. Control. Rel.* **41**: 33–48
- Guy, R. H., Kalia, Y. N., Delgado-Charro, M. B., Merino, V., López, A. Marro, A. (2000) Iontophoresis: electrorepulsion and electroosmosis. *J. Control. Release* **64**: 129–132
- Harms, H. M., Kaptaina, U., Kulpmann, W. R., Brabant, G., Hesch, R. D. (1989) Pulse amplitude and frequency modulation of parathyroid hormone in plasma. *J. Clin. Endocrinol. Metab.* **69**: 843–851
- Hock, J. M., Gera, I. (1992) Effects of continuous and intermittent administration and inhibition of resorption on the anabolic response of bone to parathyroid hormone. *J. Bone Miner. Metab. Res.* **7**: 65–72
- Iga, K., Ogawa, Y., Yashiki, T., Shimamoto, T. (1986) Estimation of drug absorption rates using a deconvolution method with nonequal sampling times. *J. Pharmacokinet. Biopharm.* **14**: 213–225
- Itagaki, S., Ishii, Y., Lee, M.-J., Doi, K. (1995) Dermal histology of hairless rat derived from Wistar strain. *Exp. Anim.* **44**: 279–284
- Kawase, M., Karino, N., Imanishi, A., Nakagawa, S., Fukuda, T., Taketomi, S., Tsuda, M. (1994) *J. Bone Miner. Met.* **12**: S27–S31
- Lindsay, R., Nieves, J., Formica, C., Henneman, E., Woelfert, L., Shen, V., Dempster, D., Cosman, F. (1997) Randomized controlled study of effect of parathyroid hormone on vertebral-bone mass and fracture incidence among postmenopausal women on estrogen with osteoporosis. *Lancet* **350**: 550–555
- Nakagawa, Tamakashi, Y., Ishibashi, Y., Kawase, M., Taketomi, S., Nishimura, O., Fukuda, T. (1994) Production of hPTH (1-34) via a recombinant DNA technique. *Biochem. Biophys. Res. Commun.* **200**: 1735–1741
- Okabe, K., Yamaguchi, H., Kawai, Y. (1986) New iontophoretic transdermal administration of beta blocker metoprolol. *J. Control. Rel.* **4**: 79–85
- Panchagnula, R., Stremmer, K., Ritschel, W. A. (1997) Animal models for transdermal drug delivery. *Meth. Find. Exp. Clin. Pharmacol.* **19**: 335–341
- Phipps, J. B., Gyory, J. R. (1992) Transdermal ion migration. *Adv. Drug. Deliv. Rev.* **9**: 137–176
- Reeve, J. (1996) PTH: a future role in the management of osteoporosis? *J. Bone Miner. Res.* **11**: 440–445
- Riond, J. L. (1993) Modulation of the anabolic effect of synthetic human parathyroid hormone fragment(1–34) in the bone of growing rats by variations in the dosage regimen. *Clin. Sci.* **85**: 223–228
- Riviere, J. E., Heit, M. C. (1997) Electrically-assisted transdermal drug delivery. *Pharm. Res.* **14**: 687–697
- Sone, T., Fukunaga, M., Ono, S., Nishiyama, T. (1995) A small dose of human parathyroid hormone(1–34) increased bone mass in the lumbar vertebrae in patients with senile osteoporosis. *Miner. Electrolyte. Metab.* **21**: 232–235
- Tam, S. C. S., Heersche, J. N. M., Murray, T. M., Parsons, J. A. (1982) Parathyroid hormone stimulates the bone apposition rate independently of its resorptive action: differential effects of intermittent and continuous administration. *Endoc.* **110**: 506–512
- Uzawa, T., Hori, M., Ejiri, S., Ozawa, H. (1995) Comparison of the effects of intermittent and continuous administration of human parathyroid hormone(1–34) on rat bone. *Bone* **16**: 477–484